AD 744 815

LINEARIZED THEORIES OF IONIZATION WAVES

THESIS

GEP/PH/72-13 Robert S. McCulloch
Captain USAF

I

Unclassified
Security Classification

DOCUMENT CONTROL DATA - R & D

(Security classification of title, body of abstract and indexing annotation must be entered when the overall report is classified)

1. ORIGINATING ACTIVITY (Corporate author) Air Force Institute of Technology (AFIT-EN) Wright-Patterson AFB, Ohio 45433	2a. REPORT SECURITY CLASSIFICATION Unclassified 2b. GROUP

3. REPORT TITLE

Linearized Theories of Ionization Waves

4. DESCRIPTIVE NOTES (Type of report and inclusive dates)

AFIT Thesis

5. AUTHOR(S) (First name, middle initial, last name)

Robert S. McCulloch
Captain USAF

6. REPORT DATE	7a. TOTAL NO. OF PAGES	7b. NO. OF REFS
June 1972	50	14

8a. CONTRACT OR GRANT NO. b. PROJECT NO. 7071-00-21 c. DoD Element 61102F d. DoD Subelement 681304	9a. ORIGINATOR'S REPORT NUMBER(S) GEP/PH/72-13 9b. OTHER REPORT NO(S) (Any other numbers that may be assigned this report)

10. DISTRIBUTION STATEMENT

Approved for public release; distribution unlimited.

11. SUPPLEMENTARY NOTES	12. SPONSORING MILITARY ACTIVITY
	Aerospace Research Laboratories (LB) Wright-Patterson AFB, Ohio 45433

13. ABSTRACT

A model for ionization waves in a D.C. gas discharge is developed in a straightforward manner based on the linearized first three moment equations for positive ions and electrons and Poisson's equation. Slab symmetry is imposed. The predictions obtained by applying this model to discharge conditions for which ionization waves have been observed are in good qualitative agreement with both the results of experiment and the predictions of other theories. The effects of including small perturbations in ion temperature and electron neutral momentum transfer collision frequency and energy transfer collision frequency are also discussed.

II

DD FORM 1 NOV 65 1473

Unclassified
Security Classification

Unclassified
Security Classification

14. KEY WORDS	LINK A		LINK B		
	ROLE	WT	ROLE	WT	RO
Ionization Waves					
Moving Striations					
Two Species Three Moment Model					
Linearized Moment Equations					
Positive Column					
D.C. Gas Discharge					

Unclassified
Security Classification

LINEARIZED THEORIES OF IONIZATION WAVES

THESIS

Presented to the Faculty of the School of Engineering

of the Air Force Institute of Technology

Air University

in Partial Fulfillment of the

Requirements for the Degree of

Master of Science

by

Robert S. McCulloch, B.S.E.S.

Captain USAF

Graduate Engineering Physics

June 1972

TV

Preface

This report represents the culmination of what has been for me a most interesting and educational research experience. I wish to thank Dr. David A. Lee, my advisor, and his staff, without whose support and guidance this would not have been possible.

Contents

List of Figures

List of Tables

Abstract

A model for ionization waves in a D.C. gas discharge is developed in a straightforward manner based on the linearized first three moment equations for positive ions and electrons and Poisson's equation. Slab symmetry is imposed. The predictions obtained by applying this model to discharge conditions for which ionization waves have been observed are in good qualitative agreement with both the results of experiment and the predictions of other theories. The effects of including small perturbations in ion temperature and electron neutral momentum transfer collision frequency and energy transfer collision frequency are also discussed.

LINEARIZED THEORIES OF IONIZATION WAVES

I. Introduction

The positive column of most D.C. gas discharges is a large luminous region lying between the anode glow at the anode and the Faraday dark space toward the cathode (Fig. 1). Often for discharge conditions of particular interest, because of their applications in laser technology, the column can be seen at any particular instant to have a regularly striated appearance (Fig. 1). When first observed these waves were somewhat of a mystery; however, in the past fifteen years several models have been proposed to describe such ionization waves. Among these are the models of Pekarek (Ref 3), Weissglas and Andersson (Ref 14), and Swain and Brown (Ref 12). The primary basis for each of these models is the use of a two species three moment treatment to describe small variations in local electric fields, number densities, drift velocities, and temperatures. These models differ in the exact form of the moment equations used and in simplifying assumptions made. This report explores the predictions of the straightforward one dimensional two species three moment model of discharge disturbances derived in Section II and, in Section III, compares these predictions with the results of experiment and with the predictions of the theories of Pekarek and Swain and Brown.

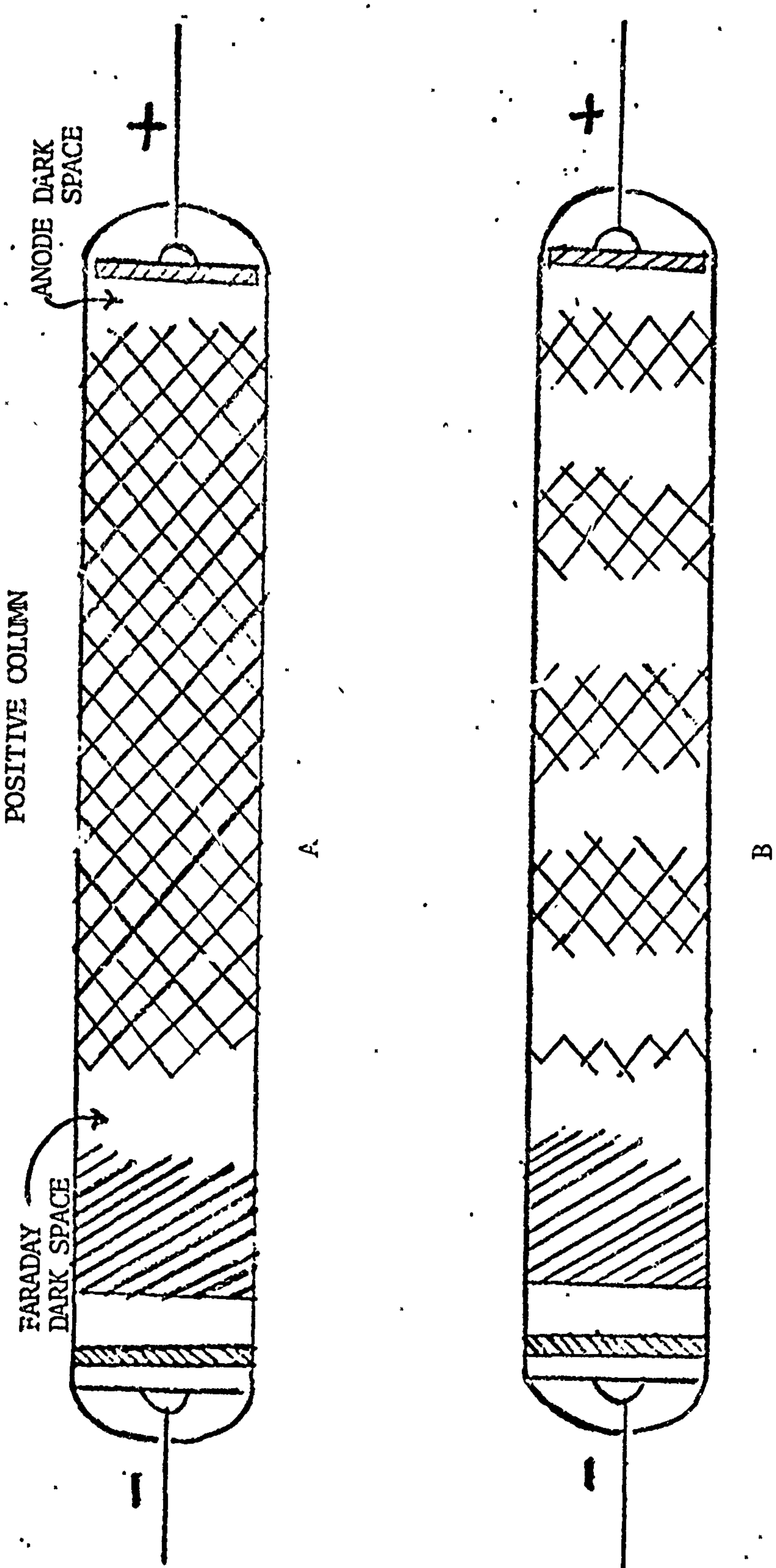

Figure 1. D.C. Gas Discharges with a Uniform Column (A) and Ionization Waves in the Column (B)

II. Theory

The Equilibrium Positive Column (Ref 2: 238-251)

This discussion of the equilibrium positive column of a gas discharge is intended to establish relationships which will prove useful in later sections. The axial electric field strength E in the column is approximately constant. A direct consequence of this, seen from the one dimensional Poisson equation

$$\frac{\partial E}{\partial x} = \frac{q_0}{\varepsilon_0}(N_i - N_e) \simeq 0 \tag{1}$$

is that electron and ion number densities, N_i and N_e respectively, are approximately equal everywhere along the longitudinal coordinate of the column x. The primary charge carrier production mechanism in the column is ionizing collisions between fast random electrons and neutrals. The primary loss mechanism of charge carriers is ambipolar flow to the walls of the tube. This ambipolar flow is set up when, prior to equilibrium, electrons, due to their greater mobility, diffuse to the tube wall much faster than positive ions. A radial field then exists such that the wall is at a negative potential with respect to the rest of the column. This field helps further induce ambipolar flow by tending to annul original differences in number density by pulling ions toward the wall and repelling electrons (Ref 2: 143-145). Current in the column is also approximately constant with most of the current being carried by the more mobile electrons. The slower positive ions, meanwhile, balance the electron space charge.

Since current is constant and there is no build up of charge in equilibrium, ionization rate must therefore balance ambipolar loss rate. Making use of this fact Von Engle arrives at the differential equation

$$\frac{d^2N}{dr^2} + \frac{1}{r}\frac{dN}{dr} + \frac{\alpha N}{D_a} = 0 \qquad (2)$$

where N represents either electron or ion number density, r represents the radial coordinate measured from the longitudinal axis of the tube, α represents ionization rate per electron, and D_a represents the coefficient of ambipolar diffusion (Ref 2: 144). The solution to Eq (2) is

$$\frac{N}{N_0} = J_0(r\sqrt{\alpha/D_a}) \qquad (3)$$

where N_0 represents the equilibrium number density along the longitudinal axis and J_0 represents the zero order Bessel function. Assuming that at the tube wall $(r = R)$, $N(R) = 0$, Eq (3) is satisfied when

$$\frac{\alpha}{D_a} = (\zeta_1/R)^2 \qquad (4)$$

where ζ_1 represents the first zero of J_0.

Electron kinetic temperature T_e can be obtained directly from Eq (4) by solving

$$\frac{Ap_0\sqrt{8q_0/\pi m_e}\, V_i^{\frac{3}{2}} X^{-\frac{1}{2}} e^{-X}}{\mu^+ \frac{V_i}{X}} = \left(\frac{\zeta_1}{R}\right)^2 \qquad (5)$$

where

$$\alpha = Ap_0\sqrt{8q_0/\pi m_e}\, V_i^{\frac{3}{2}} X^{-\frac{1}{2}} e^{-X} \quad . \tag{6}$$

$$D_a \simeq \frac{\mu_+ T_e}{q_0} = \frac{\mu_+ V_i}{X} \tag{7}$$

and

$$X = \frac{q_0 V_i}{T_e} \tag{8}$$

(see Appendix A, Eq (103)). Here A represents the slope of the ionization efficiency curve in ion pairs/m/Torr/volt, p_0 represents the pressure of the neutral gas in Torr, μ_+ represents the ion mobility in m^2/volt/sec, q_0 represents the charge of an electron in coulombs, m_e represents electron mass in kg, and V_i represents ionization potential of a neutral in volts. Once T_e is found from Eqs (5) and (8) then α can be found from Eqs (4) and (7).

Equilibrium charge conservation is represented for the column by Eq (2). The equations

$$-(+)U_{e(i)} = \mu^{-(+)}E \quad . \tag{9}$$

$$-(+)q_0 U_{e(i)} E = \kappa_{e(i)} \frac{\langle V_r \rangle_{e(i)}}{\lambda_{e(i)}} (T_{e(i)} - T_0) \tag{10}$$

express equilibrium conservation of axial momentum and energy respectively for electrons (ions) (Ref 4: 50, 61) (Ref 2: 123). In Eq (9) $U_{e(i)}$ represents electron (ion) drift velocity, $\mu^{-(+)}$ represents electron (ion) mobility, and E represents axial electric field strength. In Eq (10) $\kappa_{e(i)}$ represents the average electron (ion) energy lost to a neutral per collision, $\langle V_r \rangle_{e(i)}$ represents the average electron (ion) random velocity, $\lambda_{e(i)}$ represents the electron (ion) mean free path between collisions with neutrals, and T_0 and T_i are neutral and ion kinetic temperatures respectively. For reference in a later section Eqs (9) and (10) will appear as

$$-\frac{m_e \nu_-}{q_0} U_e = E \tag{11}$$

$$\frac{m_i \nu_+}{q_0} U_i = E \tag{12}$$

$$-q_0 U_e E = \nu_{e_0} T_e \tag{13}$$

$$q_0 U_i E = \nu_{i_0} (T_i - T_0) \tag{14}$$

where $\nu_{-(+)}$ is the electron (ion) momentum transfer collision frequency and $\nu_{e_0(i_0)}$ is the electron (ion) energy transfer collision frequency. T_0 is typically small with respect to T_e in Eq (13) and has therefore been omitted.

The Basic Physical Mechanism of Striations

According to Pekarek, the basic factors in the production of moving striations, the type of positive column ionization waves of interest in this report, are the dependence of ionization rate α on local electron temperature, the production of space charges and hence electric fields due to the different diffusion rates of electrons and ions, and the changes in local electron temperature caused by space charge fields (Ref 9: 741) (Ref 10: 893). Assuming the above mentioned dependence of α on electron temperature, the sequential interaction of the above to produce moving striations is summarized by Lee, Bletzinger, and Garscadden as follows:

> The striations are considered to occur at a sufficiently high gas pressure so that ambipolar diffusion conditions are operative. The mobility of the electrons is much larger than that of the ions and a disturbance in the concentration will, after a short time, produce a positive space charge at a region where the concentration is increased. This space-charge electric field will cause a decrease in the electron temperature (giving a dark region) in the region to the anode side of the original disturbance, consequently reducing the ion density. In turn, this dark region produces a negative space charge and an increased T_e (forming a bright region) and thus an increased n_e to its anode side. This assumption is in accord with the experimental profile of the moving striations (Ref 11: 381).

From the above explanation it is apparent that striation phenomena can be modeled as small perturbations of the ionization rate α, the charge carrier number densities N_i and N_e, electron kinetic temperature T_e, and electric field E. Axial variations in these quantities were the basis of the original Pekarek theory (Ref 6: 452). In a very recent model by Swain and Brown based on the first two ion moment equations and the first three electron moment equations, small axial perturbations of electron drift velocity U_e, ion drift velocity U_i, and ν_{e0} with respect to T_e were also considered. Swain and Brown further consider N_i always equal to N_e, assume T_i to be negligible, and allow radial variation in their basic and equilibrium equations. They, however, consider no variation in radial velocities and only wave like axial variation of the remaining quantities in their first order linearized equations. They make no attempt to perturb the ambipolar loss term (Ref 12: 1383-1386). The model discussed in the following sections is strictly a one dimensional model. In addition, N_i is not considered equal to N_e, an attempt is made to vary the ambipolar loss term, and perturbations of T_i, ν_- with respect to E, and ν_{e_0} with respect to E are considered.

The Three Moment Equations[1]

The discharge conditions and plasma oscillations discussed in this paper are limited to those for which the motion of positive ions and electrons can be adequately described by the first three moments of the Boltzmann equation. Assuming f^i the distribution function for the ith species to be isotropic in a system drifting with an average velocity $\bar{q}$, the first three moment equations for any species are

$$\frac{\partial n}{\partial t} + \frac{\partial(nq_\ell)}{\partial x_\ell} = \int_{\bar{v}} d\bar{v}\left(\frac{\partial f}{\partial t}\right)_{coll.} \tag{15}$$

$$mn\left(\frac{\partial}{\partial t} + q_j \frac{\partial}{\partial x_j}\right)q_\ell = n\langle F\rangle_\ell - \frac{\partial \sigma_{\ell j}}{\partial x_j} + m \int_{\bar{v}} d\bar{v}\, v_\ell \left(\frac{\partial f}{\partial t}\right)_{coll.}$$

$$- mq_\ell \int_{\bar{v}} d\bar{v}\left(\frac{\partial f}{\partial t}\right)_{coll.} \tag{16}$$

$$\frac{3}{2}\left(\frac{\partial}{\partial t} + q_\ell \frac{\partial}{\partial x_\ell}\right)p + \frac{5}{2}\, p\, \frac{\partial q_\ell}{\partial x_\ell} = \int_{\bar{v}} d\bar{v}\, \frac{mv^2}{2}\left(\frac{\partial f}{\partial t}\right)_{coll.} + \frac{1}{2}\, mq_\ell q_\ell \int_{\bar{v}} d\bar{v}\left(\frac{\partial f}{\partial t}\right)_{coll.}$$

$$- mq_\ell \int_{\bar{v}} d\bar{v}\, v_\ell\left(\frac{\partial f}{\partial t}\right)_{coll.} \tag{17}$$

where x_ℓ represents the position space coordinate in the ℓth direction, t represents time, $\langle F\rangle_\ell$ represents the sum of external forces averaged

[1]The treatment discussed in the remainder of this section closely parallels that of D. A. Lee (Ref 8: 1-19).

over velocity space, $\sigma_{\ell j}$ represents the kinetic stress tensor, m represents the particle mass of the species, p represents the pressure measured by an observer drifting with velocity q_ℓ,

$$q_\ell = \frac{1}{n}\int_{\bar{v}} d\bar{v}\; v_\ell f \tag{18}$$

and

$$n = \int_{\bar{v}} d\bar{v}\; f \tag{19}$$

Here the usual repeated subscript notation is used to indicate summation. Eq (16) describes momentum transfer in the ℓth direction. Assuming f to be Maxwellian, the kinetic stress tensor $\sigma_{\ell j}$ becomes

$$\sigma_{\ell j} = p\delta_{\ell j} = nT\delta_{\ell j} \tag{20}$$

where T is the kinetic temperature of the species (Ref 1: 114-121). If there is no applied magnetic field, the self field is neglected with respect to the applied electric field in the Lorentz force term, and all other forces are neglected, then $\langle F\rangle_\ell$ reduces to zq_0E_ℓ where z represents charge number and sign, q_0 represents basic electronic charge and E_ℓ represents the ℓth component of electric field strength. With these assumptions and letting

$$Q = \int_{\bar{v}} d\bar{v}\left(\frac{\partial f}{\partial t}\right)_{\text{coll.}} \tag{21}$$

$$nA_\ell = \int_{\bar{v}} d\bar{v}\; v_\ell\left(\frac{\partial f}{\partial t}\right)_{\text{coll.}} \tag{22}$$

$$nP = \frac{m}{2}\int_{\bar{v}} d\bar{v}\; v_\ell v_\ell\left(\frac{\partial f}{\partial t}\right)_{\text{coll.}} \tag{23}$$

Eqs (15), (16), and (17) can be written with slight simplification as:

$$\frac{\partial n}{\partial t} + \frac{\partial (nq_\ell)}{\partial x_\ell} = Q \tag{24}$$

$$\frac{\partial q_\ell}{\partial t} + q_j \frac{\partial q_\ell}{\partial x_j} = -\frac{1}{n}\frac{\partial}{\partial x_\ell}\left(\frac{nT}{m}\right) + \frac{zq_0 E_\ell}{m} + A_\ell - \frac{Q}{n} q_\ell \tag{25}$$

$$\frac{\partial T}{\partial t} + q_\ell \frac{\partial T}{\partial x_\ell} = -\frac{2}{3} T\frac{\partial q_\ell}{\partial x_\ell} - \frac{2}{3} mA_\ell q_\ell + \frac{2}{3} P + \frac{Q}{n}\left(q_\ell q_\ell \frac{m}{3} - T\right) \tag{26}$$

Moving striations propagate longitudinally in the positive column. In order to simplify Eqs (24), (25), and (26) variations in $\overline{q}$, $\overline{E}$ and $\overline{x}$ will be considered to take place only in the longitudinal or x direction where x increases from anode to cathode. This is not of course a good assumption in terms of what is actually happening in the column since radial variations in charge carrier velocity and electric field strength exist and undoubtedly have their effect on local electron temperature and particle production and loss. However, the solution of the much simpler one dimensional equations does provide qualitative results and an insight into the more complex three dimensional problem. Thus, letting $\overline{q} = \{u,0,0\}$, $\overline{E} = \{E,0,0\}$, and $\overline{x} = \{x,0,0\}$ Eqs (24), (25), and (26) become

$$\frac{\partial N_e}{\partial t} + N_e \frac{\partial U_e}{\partial x} + U_e \frac{\partial N_e}{\partial x} = Q \tag{27}$$

$$\frac{\partial N_i}{\partial t} + N_i \frac{\partial U_i}{\partial x} + U_i \frac{\partial N_i}{\partial x} = Q \tag{28}$$

$$\frac{\partial U_e}{\partial t} + U_e \frac{\partial U_e}{\partial x} + \frac{T_e}{N_e m_e}\frac{\partial N_e}{\partial x} + \frac{1}{m_e}\frac{\partial T_e}{\partial x} = -\frac{q_0 E}{m_e} + A_e + \frac{QU_e}{N_e} \tag{29}$$

$$\frac{\partial U_i}{\partial t} + U_i \frac{\partial U_i}{\partial x} + \frac{T_i}{N_i m_i} \frac{\partial N_i}{\partial x} + \frac{1}{m_i} \frac{\partial T_i}{\partial x} = \frac{Zq_0 E}{m_i} + A_i + \frac{QU_i}{N_i} \tag{30}$$

$$\frac{\partial T_e}{\partial t} + U_e \frac{\partial T_e}{\partial x} + \frac{2}{3} T_e \frac{\partial U_e}{\partial x} = -\frac{2}{3} m_e \Lambda_e U_e + \frac{2}{3} P_e + Q\left(\frac{m_e U_e^2}{3} - T_e\right) \tag{31}$$

$$\frac{\partial T_i}{\partial t} + U_i \frac{\partial T_i}{\partial x} + \frac{2}{3} T_i \frac{\partial U_i}{\partial x} = -\frac{2}{3} m_i \Lambda_i U_i + \frac{2}{3} P_i + Q\left(\frac{m_i U_i^2}{3} - T_i\right) \tag{32}$$

Eqs (27)-(32) along with Poisson's equation

$$\frac{\partial E}{\partial x} = \frac{q_0}{\varepsilon_0} (ZN_i - N_e) \tag{33}$$

are a system of first order non-linear differential equations relating N_e, N_i, U_e, U_i, T_e, T_i, and E. The subscripts i and e denote ion and electron quantities respectively.

The Collision Terms

Q represents particle production and loss due to collisions. As previously mentioned, the primary charge carrier production mechanism is ionizing collisions between fast electrons and neutrals. This is just simply the rate of ionization per electron times electron number density or αN_e. Since the primary charge carrier loss mechanism, ambipolar flow to the walls, is a radial phenomenon, no realistic charge loss model is available. In order to balance charge production and charge loss in equilibrium a contrived loss term $-\frac{1}{\tau}(N_i + N_e)$, similar to that used by Pekarek, is included in this analysis (Ref 3: 857). Here τ represents the mean life time of the charge carriers. τ probably depends upon both α and T_e, however, since the nature of this dependence is unknown, it will be considered constant throughout this treatment. Hence,

$$Q = \alpha N_e - \frac{1}{\tau}(N_i + N_e) \tag{34}$$

In equilibrium the acceleration of the electrons (ions) by the applied electric field must be equal to the rate of their momentum transfer to neutrals during collisions. Hence from Eqs (29) and (30)

$$A_e \overset{m}{=} \frac{q_0 E}{m_e} \tag{35}$$

$$A_i \overset{m}{=} - \frac{Zq_0 E}{m_i} \tag{36}$$

Therefore from Eqs (11) and (12)

$$A_e = -\nu_- U_e \tag{37}$$

$$A_i = -\nu_+ U_i \tag{38}$$

In equilibrium Eqs (31) and (32) combined with Eqs (35) and (36) become

$$q_0 E U_e = m_e A_e U_e = P_e \tag{39}$$

$$-Zq_0 E U_i = m_i A_i U_i = P_i \tag{40}$$

Therefore from Eqs (13) and (14)

$$P_e = -\nu_{e_0} T_e \tag{41}$$

$$P_i = -\nu_{i_0}(T_i - T_0) \tag{42}$$

The Characteristic Form of the Equations

With the collision terms modeled as in the previous section, Eqs (27) and (33) are a system of quasi-linear equations having the form

$$A_{ij}\frac{\partial y_j}{\partial x} + B_{ij}\frac{\partial y_i}{\partial t} = F_i \tag{43}$$

where A_{ij}, B_{ij} and F_i are functions of the variables y_j. The equations of such a system can be written as an equivalent system of equations each of which involves differentiation in only one direction in the x-t plane at each point (x,t), provided there exist j vectors $V = V_i$, i = 1, ..., j, such that j linear combinations of system (42) of the form

$$V_i A_{ij}\frac{\partial y_j}{\partial x} + V_i B_{ij}\frac{\partial y_i}{\partial t} = V_i F_i \tag{44}$$

exist where

$$V_i A_{ij} = \lambda V_i B_{ij} \tag{45}$$

for real λ. If j such linear combinations do exist, then these equations can be used to form an equivalent system of equations each having the characteristic form

$$\left(\lambda\frac{\partial y_j}{\partial x} + \frac{\partial y_i}{\partial t}\right)V_i B_{ij} = V_i F_i \tag{46}$$

where the differentiation is in one direction only, along the curve $(x - x_0) = \lambda(t - t_0)$ (Ref 5: 103-107) (Ref 8: 10).

The λ's associated with the system (27)-(32) are U_e, $U_e \pm a_e$, U_i and $U_i \pm a_i$ where $a_e = \sqrt{\frac{5}{3}T_e/m_e}$ and $a_i = \sqrt{\frac{5}{3}T_i/m_i}$. Eqs (27)-(33) written in characteristic form are:

$$-\frac{2}{3}T_e\frac{\partial N_e}{\partial s_e}+N_e\frac{\partial T_e}{\partial s_e}=-\frac{5}{3}T_eQ+\frac{2}{3}\left(P_e-m_eA_eU_e+\frac{m_e}{2}\frac{Q}{N_e}U_e^{\,2}\right)N_e \quad (47)$$

$$-\frac{2}{3}T_i\frac{\partial N_i}{\partial s_i}+N_i\frac{\partial T_i}{\partial s_i}=-\frac{5}{3}T_iQ+\frac{2}{3}\left(P_i-m_iA_iU_i+\frac{m_i}{2}\frac{Q}{N_i}U_i^{\,2}\right)N_i \quad (48)$$

$$\frac{T_e}{m_e}\frac{\partial N_e}{\partial\lambda_e^{\pm}}\pm N_ea_e\frac{\partial U_e}{\partial\lambda_e^{\pm}}+\frac{N_e}{m_e}\frac{\partial T_e}{\partial\lambda_e^{\pm}}=\mp N_ea_e\left(\frac{q_0E}{m_e}-A_e+\frac{QU_e}{N_e}\right)-\frac{2}{3}N_eA_eU_e+\frac{2}{3}\frac{N_eP_e}{m_e}$$

$$+\frac{Q}{3}U_e^{\,2} \quad (49)\text{ and }(50)$$

$$\frac{T_i}{m_i}\frac{\partial N_i}{\partial\lambda_i^{\mp}}\pm N_ia_i\frac{\partial U_i}{\partial\lambda_i^{\mp}}+\frac{N_i}{m_i}\frac{\partial T_i}{\partial\lambda_i^{\mp}}=\pm N_ia_i\left(\frac{Zq_0E}{m_i}+A_i-\frac{QU_i}{N_i}\right)-\frac{2}{3}N_iA_iU_i+\frac{2}{3}\frac{N_iP_i}{m_i}$$

$$+\frac{Q}{3}U_i^{\,2} \quad (51)\text{ and }(52)$$

where $\frac{\partial}{\partial s_{e(i)}}=\frac{\partial}{\partial t}+U_{e(i)}\frac{\partial}{\partial x}$ and $\frac{\partial}{\partial\lambda^{\pm}_{e(i)}}=\frac{\partial}{\partial t}+(U_{e(i)}\pm a_{e(i)})\frac{\partial}{\partial x}$. Poisson's Eq (33) is in characteristic form.

The Simplified Electron Equations

In the electron equations the time derivatives may be neglected for any electron variable Y_e since for phenomena of interest

$$\left|\frac{\partial Y_e}{\partial t}\right| << \left|U_e\frac{\partial Y_e}{\partial x}\right| << \left|(U_e\pm a_e)\frac{\partial Y_e}{\partial x}\right| \quad (53)$$

(Ref 6: 454). This is equivalent to saying that both the electron drift velocity U_e which is usually $\geq 10^3$m/sec and the electron acoustic speed a_e usually $> 10^5$m/sec are much greater than the phase velocity of the ionization waves which is usually $< 10^2$m/sec. Making use of statement

(53) and using the fact that $U_e^2 \ll a_e^2$, Eqs (47), (49), and (50) can be reduced to

$$\frac{\partial N_e}{\partial x} = \frac{2}{5}\frac{\nu_{e0}N_e}{U_e} - m_e\frac{\nu_- U_e N_e}{T_e} - \frac{3}{5}q_0 E N_e + \left[\alpha N_e - \frac{1}{\tau}(N_i + N_e)\right]\frac{1}{U_e} \tag{54}$$

$$\frac{\partial U_e}{\partial x} = \frac{\nu_- U_e^2 m_e}{T_e} - \frac{2}{5}\nu_{e0} + \frac{3}{5}\frac{q_0 E U_e}{T_e} + \frac{4}{5}\left[\alpha N_e - \frac{1}{\tau}(N_i + N_e)\right]\frac{U_e^2 m_e}{N_e T_e} \tag{55}$$

$$\frac{\partial T_e}{\partial x} = -\frac{2}{5}\frac{\nu_{e0}T_e}{U_e} - \frac{2}{5}q_0 E - \left[\alpha N_e - \frac{1}{\tau}(N_i + N_e)\right]\frac{T_e}{U_e N_e} \tag{56}$$

where the relationships expressed by Eqs (34), (37), and (41) have been substituted for Q, A_e, and P_e respectively.

The Nondimensional Linearized Electron Equations

In a normal equilibrium discharge N_e, N_i, U_e, U_i, T_e, T_i and E are approximately constant. Thus the equilibrium conditions resulting from Eqs (33), (54), (55), and (56) are

$$N_i = N_e = N^0 \tag{57}$$

$$\alpha = \frac{2}{\tau} \tag{58}$$

$$\frac{\nu_{e0}T_e^0}{U_e^0} = -q_0 E^0 = \nu_- U_e^0 m_e \tag{59}$$

where the zero superscript denotes equilibrium value. Since no radial variation in number density is allowed, N^0, the average number density in any cross section of the column, is taken for the equilibrium number density for both electrons and ions throughout the column. The variables N_i, N_e, U_e, T_e and E are assumed to have the following form: $Y = Y^0 + y\exp(ikx + st)$ where Y represents any one of the above mentioned variables, Y^0 its equilibrium value, and $y\exp(ikx + st)$ a small perturbation of Y away from the equilibrium value with variation in space and time as indicated.

As previously mentioned α may be considered to vary with T_e, ν_- with E, and ν_{e_0} with both T_e and E; therefore, small perturbations in these appear here as

$$\alpha = \alpha + \alpha' \, te \tag{60}$$

$$\nu_- = \nu_- + \dot{\nu}_- \, e \tag{61}$$

$$\nu_{e_0} = \nu_{e_0} + \dot{\nu}_{e_0} \, e + \nu'_{e_0} \, te \tag{62}$$

where ' (prime) denotes $\left.\frac{\partial}{\partial T_e}\right|_{T_e=T_e{}^0}$ and $\cdot$ (dot) denotes $\left.\frac{\partial}{\partial E}\right|_{E=E^0}$. α' can be computed directly from Eq (6). Swain and Brown (Ref 12: 1383-1386) consider ν_- constant; however, according to Von Engle

$$\mu_- \propto E^{-\frac{1}{2}} \tag{63}$$

when equilibrium discharge conditions are such that collisions between electrons and neutrals may be considered elastic (Ref 2: 124). This variation can be used provided the time to reach microscopic equilibrium (approximately 10^{-6} sec) is short compared with the period of oscillation of striations (approximately 10^{-3} sec). For elastic collisions based on statement (63)

$$\dot{\nu}_{-} = \frac{1}{2}\frac{1}{E^0}\nu_{-} \tag{64}$$

For inelastic collisions ν_- will be approximated as constant; hence $\dot{\nu}_- = 0$. Plots available in the literature similar to that in Fig. 2 are used to determine which type of variation is appropriate for a particular gas and discharge condition (see Table I). Based on Eqs (10) and (13)

$$\nu_{e_0} = \kappa\frac{\langle V_{r_e}\rangle}{\lambda_e} = \kappa\frac{\sqrt{2/m_e}}{\lambda_e}T_e^{\frac{1}{2}} \tag{65}$$

From Eq (65)

$$\nu'_{e_0} = \frac{1}{2}\frac{\nu_{e_0}}{T_e^{\,0}} \tag{66}$$

and

$$\dot{\nu}_{e_0} = \frac{1}{\kappa}\dot{\kappa}\nu_{e_0} \tag{67}$$

Electron mean free path λ_e is approximately constant for discharge conditions of interest here (Ref 2: 33, 34). For elastic electron-neutral collisions, the fraction of energy transferred κ is constant and $\dot{\nu}_{e_0} = 0$. Plots available in the literature similar to that in Fig. 3 are used to determine which type variation is appropriate for particular gas and discharge conditions (see Table I).

With the above assumptions the linearized nondimensional electron equations are

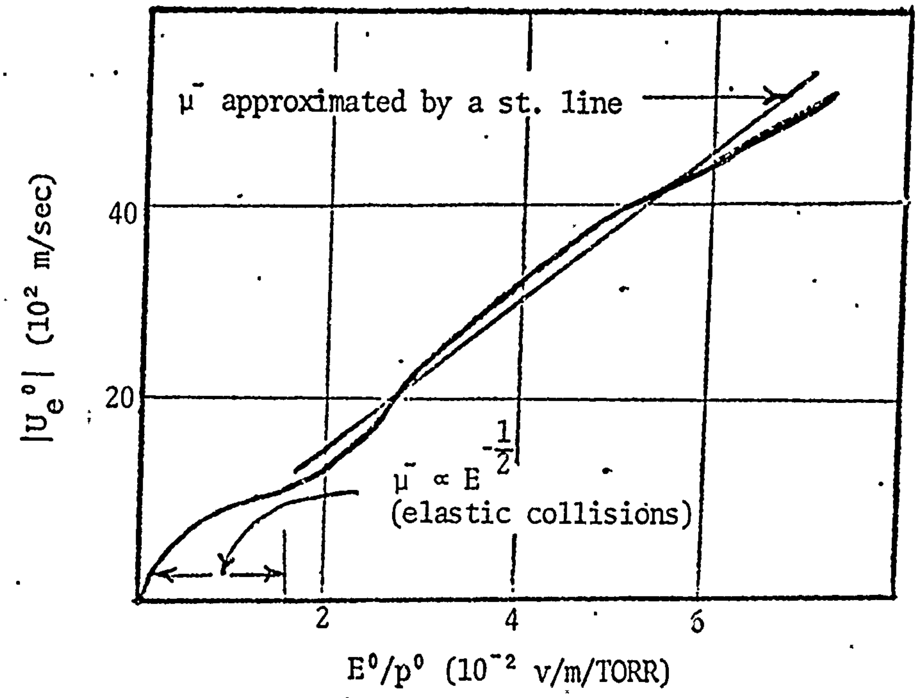

Figure 2. An Example of Equilibrium Electron Drift Velocity $|U_e{}^o|$ as a Function of Reduced Field E^o/p^o for an Arbitrary Gas.

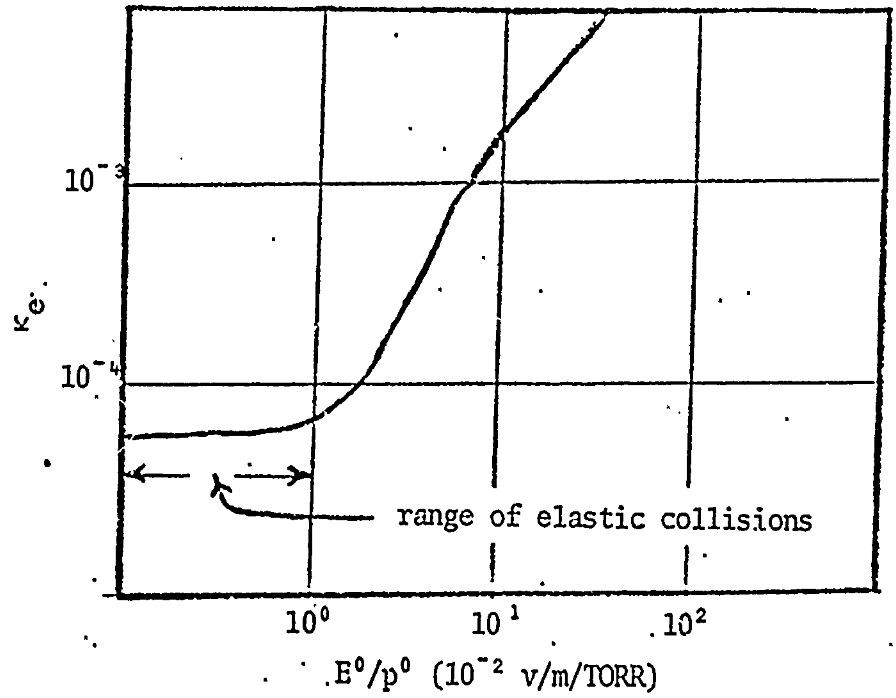

Figure 3. An Example of Equilibrium Average Fraction of Energy Transferred per Electron-Neutral Collision κ_e as a Function of Reduced Field for the Same Arbitrary Gas.

$$ikn_e = \left(\frac{3}{5}a + \alpha_e'^*\right)t_e - \frac{7}{5}au_e + \frac{1}{10}ae - \frac{1}{\tau_e^*}(n_i - n_e) \tag{68}$$

$$iku_e = \left(-\frac{3}{5}a + \frac{4}{5}\alpha_e'^*\mu_e^2\right)t_e + \frac{7}{5}au_e - \frac{1}{10}ae - \frac{4}{5}\frac{\mu_e^2}{\tau_e^*}(n_i - n_e) \tag{69}$$

$$ikt_e = \left(-\frac{3}{5}a - \alpha_e'^*\right)t_e + \frac{2}{5}au_e + \frac{2}{5}ae + \frac{1}{\tau_e^*}(n_i - n_e) \tag{70}$$

for discharge conditions such that momentum and energy are transferred through elastic collisions and

$$ikn_e = \left(\frac{3}{5}a + \alpha_e'^*\right)t_e - \frac{7}{5}au_e + \left(\frac{3}{5}a + \frac{2}{5}a\dot{\kappa}^*\right)e - \frac{1}{\tau_e^*}(n_i - n_e) \tag{71}$$

$$iku_e = \left(-\frac{3}{5}a + \frac{4}{5}\alpha_e'^*\mu_e^2\right)t_e + \frac{7}{5}au_e - \left(\frac{3}{5}a + \frac{2}{5}a\dot{\kappa}^*\right)e - \frac{4}{5}\frac{\mu_e^2}{\tau_e^*}(n_i - n_e) \tag{72}$$

$$ikt_e = \left(-\frac{3}{5}a - \alpha_e'^*\right)t_e + \frac{2}{5}au_e + \left(\frac{2}{5}a - \frac{2}{5}a\dot{\kappa}^*\right)e + \frac{1}{\tau_e^*}(n_i - n_e) \tag{73}$$

for discharge conditions such that momentum and energy are transferred through inelastic collisions. The nondimensional quantities, except a, in the above are the variables x, k, n_e, n_i, and t_e denoting $\frac{x}{R}$, kR, $\frac{n_e}{N^0}$, $\frac{n_i}{N^0}$, $\frac{u_e}{U_e{}^0}$, and $\frac{t_e}{T_e{}^0}$ respectively and the nondimensional constants $\alpha_e'^*$, τ_e^*, $\dot{\kappa}^*$, and μ_e denoting $\alpha' \frac{T_e{}^0 R}{U_e{}^0}$, $\tau_e \frac{U_e{}^0}{R}$, $\frac{E^0}{\kappa}\dot{\kappa}$, and $\sqrt{U_e{}^{0\,2} m_e / T_e{}^{0\,2}}$ respectively. The constant a is defined by the equations

$$a = \frac{\nu_{e_0} R}{U_e^{\,0}} = -\frac{q_0 E^0 R}{T_e^{\,0}} = \frac{m_e U_e^{\,0} R}{T_e^{\,0}} \nu_- \tag{74}$$

The R appearing in the above quantities denotes tube radius.

The Nondimensional Linearized Ion Equations

In addition to Eqs (57) and (58) the ion equilibrium equations resulting from (33), (48), (51), and (52) are:

$$q_0 E^0 = \nu_+ u_i^{\,0} m_i = \frac{\nu_{i_0}(T_i^{\,0} - T_0)}{U_i^{\,0}} \tag{75}$$

Assume the variables N_i, N_e, U_i, and T_i also vary as $Y = Y^0 + y\exp(ikx + st)$ as in the case of the electron variables. ν_+ and ν_{i_0} do not vary with E since μ_+ and the fraction of energy transferred through collisions are constant for ions (Ref 2: 113, 114). Any variation of ν_{i_0} with respect to T_i is small and can be neglected based on the following:

$$-\delta P_i = \delta[\nu_{i_0}(T_i - T_0)] = \nu_{i_0} t_i + \left.\frac{\partial \nu_{i_0}}{\partial T_i}\right|_{T_i = T_i^{\,0}} (T_i^{\,0} - T_0) t_i =$$

$$\left[\nu_{i_0} + \frac{1}{2}\nu_{i_0}\left(1 - \frac{T_0}{T_i^{\,0}}\right)\right] t_i \simeq \nu_{i_0} t_i \tag{76}$$

With the above assumptions the linearized nondimensional ion equations are:

$$-\frac{2}{3}(ik + s)n_i + (ik + s)t_i = -\frac{2}{3} f t_i + \frac{4}{3} b u_i - \left(\frac{5}{3} - \frac{5}{9}\mu_i^{\,2}\right)\alpha_i^{!*} t_e$$

$$+ \left(\frac{5}{3} - \frac{5}{9}\mu_i^{\,2}\right)\frac{1}{\tau_i^*}(n_i - n_e) \tag{77}$$

$$\left[s + \left(1 \pm \frac{1}{\mu_i}\right)ik\right]n_i \pm \frac{5}{3}\mu_i\left[s + \left(1 \pm \frac{1}{\mu_i}\right)ik\right]u_i + \left[s + \left(1 \pm \frac{1}{\mu_i}\right)ik\right]t_i =$$

$$\pm \frac{b}{\mu_i} e + \left(\frac{4}{3} \mp \frac{1}{\mu_i}\right)bu_i - \frac{2}{3} ft_i$$

$$+ \left(\frac{5}{3}\mu_i^2 \mp \frac{5}{3}\mu_i\right)\left[\alpha_i'^{*}t_e + \frac{1}{\tau_i^*}(n_i - n_e)\right] \qquad (78) \text{ and } (79)$$

The nondimensional variables t, s, u_i, and t_i are respectively $t\frac{U_i^0}{R}$, $s\frac{R}{U_i^0}$, $\frac{u_i}{U_i^0}$, and $\frac{t_i}{T_i^0}$. Except for b, the nondimensional constants f, $\alpha_i'^{*}$, τ_i^*, and μ_i in the above equations are $\frac{\nu_{i_0} R}{U_i^0}$, $\frac{\alpha R T_e^0}{U_i^0}$, $\frac{\tau U_i^0}{R}$, and $\frac{U_i^0}{\sqrt{\frac{5}{3} T_i^0/m_i}}$ respectively.

$$b = \frac{\nu_+ m_i U_i^0 R}{T_i^0} = \frac{q_0 E^0 R}{T_i^0} \qquad (80)$$

The linearized, nondimensional Poisson's equation is

$$ik\varepsilon e = n_i - n_e \qquad (81)$$

where ε is $\frac{\varepsilon_0 E^0}{Rq_0 N^0}$.

The Dispersion Relation

The electron equations either Eqs (68), (69), and (70) or (71), (72), and (73) and Eq (81) are solved simultaneously to find t_e and e in terms of n_i such that

$$t_e = C_1(k)n_i \qquad (82)$$

$$e = C_2(k)n_i \tag{83}$$

where C_1 and C_2 are complex. Eqs (77), (78), (79), and (81) can be reduced to

$$\left[\frac{5}{3}s + \frac{5}{3}ik - \left(\frac{5}{3} - \frac{5}{9}\mu_i^2\right)\left(\alpha_i'^*C_1 - \frac{5}{3}C_2\frac{ik\varepsilon}{\tau_i^*}\right)\right]n_i + \frac{4}{3}bu_i + \left(-\frac{2}{3}f - ik - s\right)t_i = 0 \tag{84}$$

$$\left(s + ik - \frac{5}{9}\mu_i^2\alpha_i'^*C_1 + \frac{5}{9}\mu_i^2\frac{ik\varepsilon C_2}{\tau_i^*}\right)n_i + \left(\frac{5}{3}ik - \frac{4}{3}b\right)u_i + \left(\frac{2}{3}f + ik + s\right)t_i = 0 \tag{85}$$

$$\left[\frac{ik}{\mu_i} - \frac{b}{\mu_i}C_2 + \frac{5}{3}\mu_i\left(\alpha_i'^*C_1 - \frac{ik\varepsilon C_2}{\tau_i^*}\right)\right]n_i + \left(\frac{5}{3}\mu_i s + \frac{5}{3}ik\mu_i + \frac{b}{\mu_i}\right)u_i + \frac{ik}{\mu_i}t_i = 0 \tag{86}$$

This system has a solution only for those combinations of s and k which make the determinant of the matrix of coefficients zero (Ref 7: 157). By setting

$$\begin{vmatrix} \left[\frac{5}{3}s + \left(\frac{5}{3}ik - \frac{5}{3}\alpha_i'^*C_1 + \frac{5}{3}C_2\frac{ik\varepsilon}{\tau_i^*}\right)\right] & \left[\frac{5}{3}ik\right] & 0 \\ \left[s + \left(ik - \frac{5}{9}\mu_i^2\alpha_i'^*C_1 + \frac{5}{9}\mu_i^2\frac{ik\varepsilon C_2}{\tau_i^*}\right)\right] & \left[\frac{5}{3}ik - \frac{4}{3}b\right] & \left[s + \left(ik + \frac{2}{3}f\right)\right] \\ \left[\frac{ik}{\mu_i} - \frac{b}{2}C_2 + \frac{5}{3}\mu_i\left(\alpha_i'^*C_1 - \frac{ik\varepsilon C_2}{\tau_i^*}\right)\right] & \left[\frac{5}{3}\mu_i s + \left(\frac{5}{3}\mu_i ik + \frac{b}{\mu_i}\right)\right] & \left[\frac{ik}{\mu_i}\right] \end{vmatrix} = 0 \tag{87}$$

a dispersion relation of form

$$D(s,k) = s^3 + B(k)s^2 + C(k)s + D(k) = 0 \tag{88}$$

is obtained where B, C, and D are complex.

Striation-like behavior can be inferred where real s(k) has a positive maximum (the s(k) at which disturbances are propagated exponentially at their maximum rate) or where real s(k) has a relative negative maximum, which would indicate only slight damping (the s(k) at which disturbances are the least damped exponentially relative to those around them but not so heavily damped as to be undetectable). The phase velocity $-\frac{\mathrm{Im}(s)}{k}$ and group velocity $-\frac{\partial \mathrm{Im}(s)}{\partial k}$ as well as frequency $-\frac{\mathrm{Im}(s)}{2\pi}$ and wavelength $\frac{2\pi}{k}$ at the point of the striation-like behavior can then be computed from the dispersion relation and compared with experimental results.

The Equilibrium Data

To solve the dispersion relation Eq (87), it is necessary to compute the nondimensional constants κ^*, a, b, f, $\alpha_e'^*$, $\alpha_i'^*$, τ_e^*, τ_i^*, μ_i and μ_e from the equilibrium values E^0, p^0, N^0, U_i^0, U_e^0, T^0, T_e^0, T_i^0, ν_-, ν_+, ν_{e_0}, ν_{i_0}, α, τ, α', and R. These values, all of which are in mks units unless otherwise specified, are obtained for this treatment from a combination of experimental data, basic theory, and the equilibrium equations themselves. The gas, N^0, T^0, R, and p_0 are known or assumed based on typical experimental values. Listed in Table I are quantities useful in computing gas discharge equilibrium conditions which can be found in Von Engle (Ref 2).

Table I

Quantities Useful in Computing Gas Discharge Equilibrium Conditions

Quantity	Symbol	Units	Source (Ref 2)
Ion Mobility at 1 Torr °C	μ_0^+	$10^{-1}m^2$/sec/volt	Table 4.1, p 114
Axial Electric Field Strength	E^0	volt/m	Fig. 125, p 245; Fig. 127, p 247
Slope of Ionization Efficiency	A	ion pairs/m/Torr/volt/electron	Table 3.7, p 63
Electron drift velocity	U_e	10^3m/sec	Fig. 61, p 124
Ionization Potential	V_i	volts	Table 3.6, p 59
Fraction of energy transferred/electron neutral collision	κ		Fig. 63, p 126
	$\frac{\partial\kappa}{\partial E}$	m/volt	Fig. 63, p 126

Another excellent source for basic equilibrium data is Brown (Ref 4).

The ion mobility at 1 Torr and 0°C μ_0^+ adjusted for temperature and pressure according to the equation

$$\mu^+ = \mu_0^+ \frac{T_0}{273} \frac{1}{p_0} \qquad (89)$$

can be used to obtain ν_+ and U_i^0 from Eqs (9) and (12) when E^0 is known experimentally. The empirical formula

$$\nu_{i_0} = (7 \times 10^6)p_0 \tag{90}$$

is used to obtain ν_{i_0}. With ν_{i_0}, T^0, U_i^0, and E known T_i^0 is available from Eq (14).

From Von Engle U_e^0 can be found knowing E^0 and p^0 (see Table I). The electron mobility and hence ν_- may then be found from Eqs (9) and (11). T_e^0, α, and α' can be obtained from Eqs (5), (6), and (8) by making use of Von Engle (see Table I) to obtain A and V_i. With ν_-, E^0, U_e^0, and T_e^0 now known, ν_{e_0} is easily found from Eq (13). From Eq (58), $\tau = \frac{2}{\alpha}$. See Appendix B for sample calculation of equilibrium data.

The Method of Solution

To solve the dispersion relation Eq (87) k is assumed to be positive real. Starting with some initial value of k, numerical values for C_1 and C_2 in Eqs (82) and (83) are determined by solving simultaneously Poisson's Eq (81) and the electron equations either (68), (69), (70) or (71), (72), and (73) depending upon whether the value of E^0/p^0 was such that inelastic collisions are important. Knowing the values of k, C_1, and C_2, numerical values for each element of the determinant in Eq (87) are found. Evaluating this determinant at this point, values for B, C, and D in Eq (88) are obtained. Knowing its coefficients, the cubic dispersion relation is then solved by Newton's Method to find the first of its three complex roots. The quadratic formula is then used to find the other two roots. k is then incremented to a new value and the above process is repeated. k is most conveniently varied so that the results are easily plotted logarithmically. By using electron Eqs (71), (72), and (73) and setting $\dot{\kappa}^* = 0$ the effect of not allowing ν_- and ν_{e_0} to vary with E is easily evaluated.

III. Results

The Roots of the Dispersion Relation

The real and imaginary parts of the solutions to the dispersion relation Eq (87) for a mercury-argon discharge at 3 Torr (corresponding roughly to the experiment described in Lee *et al.* (Ref 11: 378)) are shown in Figs. 4 and 5 respectively. The equilibrium data used to model this 3 Torr mercury-in-argon case is included as a sample calculation in Appendix B. Roots a and c are heavily damped over the entire range of k. Root b, however, exhibits a negative maximum at approximately k = 3. The narrow band of frequencies around this point are those for which disturbances are the least damped and therefore the most likely to propagate. If the damping or amplification per cycle, $2\pi\left|\frac{\mathrm{Re}(s)}{\mathrm{Im}(s)}\right|$, is less than one, a wave will be considered to be neutrally damped since for such waves there is a high possibility that damping or amplification may appear as a result of the rather crude approximations used to obtain the equilibrium conditions of the discharge modeled and not as a result of the model itself. In fact, highly believable adjustments to the starting conditions for the cases examined here will actually cause the model to predict $2\pi\left|\frac{\mathrm{Re}(s)}{\mathrm{Im}(s)}\right|$ much less than one or actual neutral damping. Nevertheless, the damping per cycle predicted by the model in this case is 1.34, which even by the above criteria, indicates the presence of significant damping. The striation frequency and wavelength at the point of least damping are 8.7 khz and 1.8 cm respectively. Striation phase and group velocities, v_p and v_g, are 162 m/sec and -253 m/sec respectively. The wave predicted is a backward wave since the phase and group velocities are in opposite directions. The experimental values of v_p and v_g are

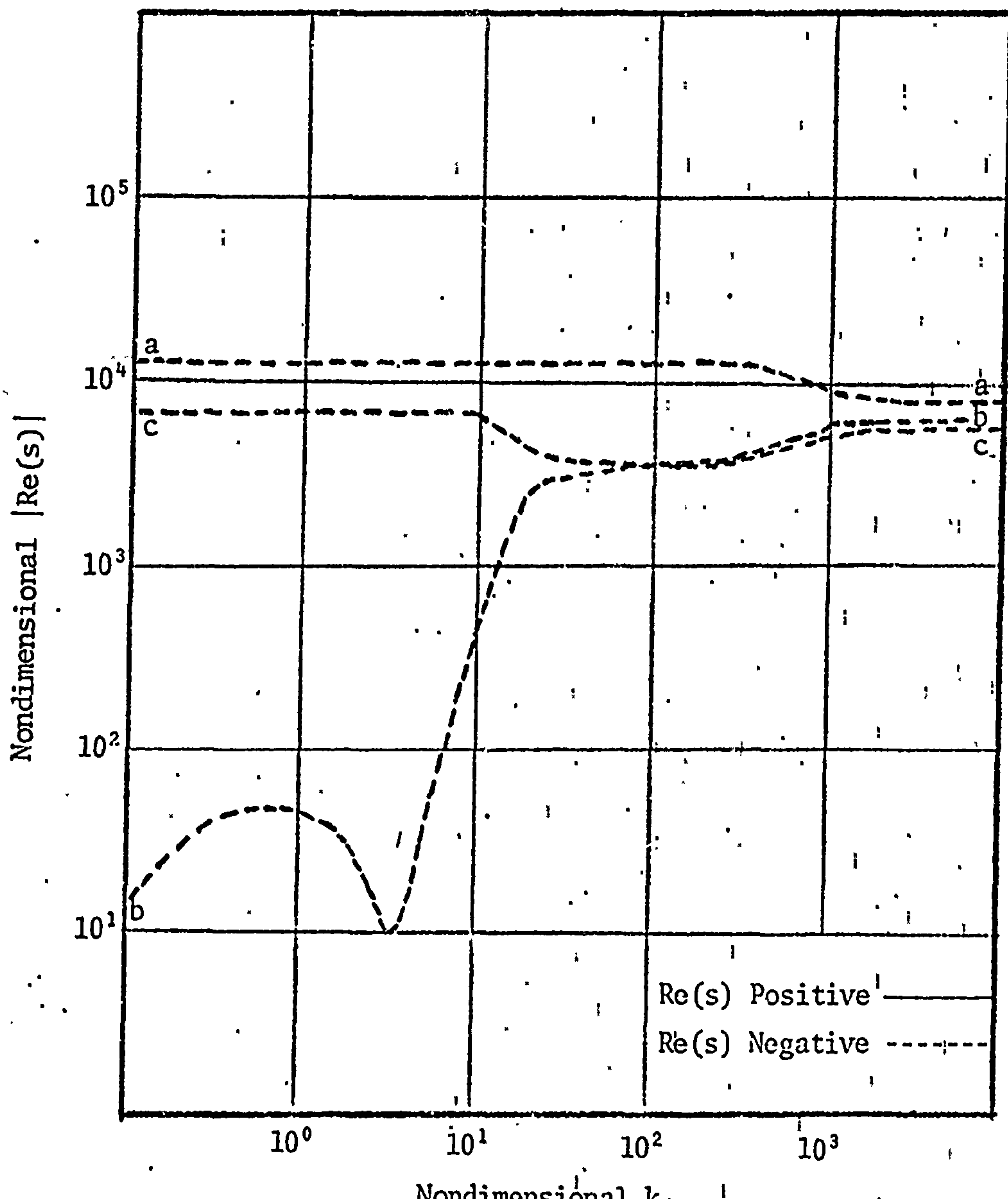

Figure 4. The Roots of the Dispersion Relation (Re(s) vs k) for the Section II Model with $\nu_- = \nu_-(E)$ (Mercury-in-Argon at 3 Torr)

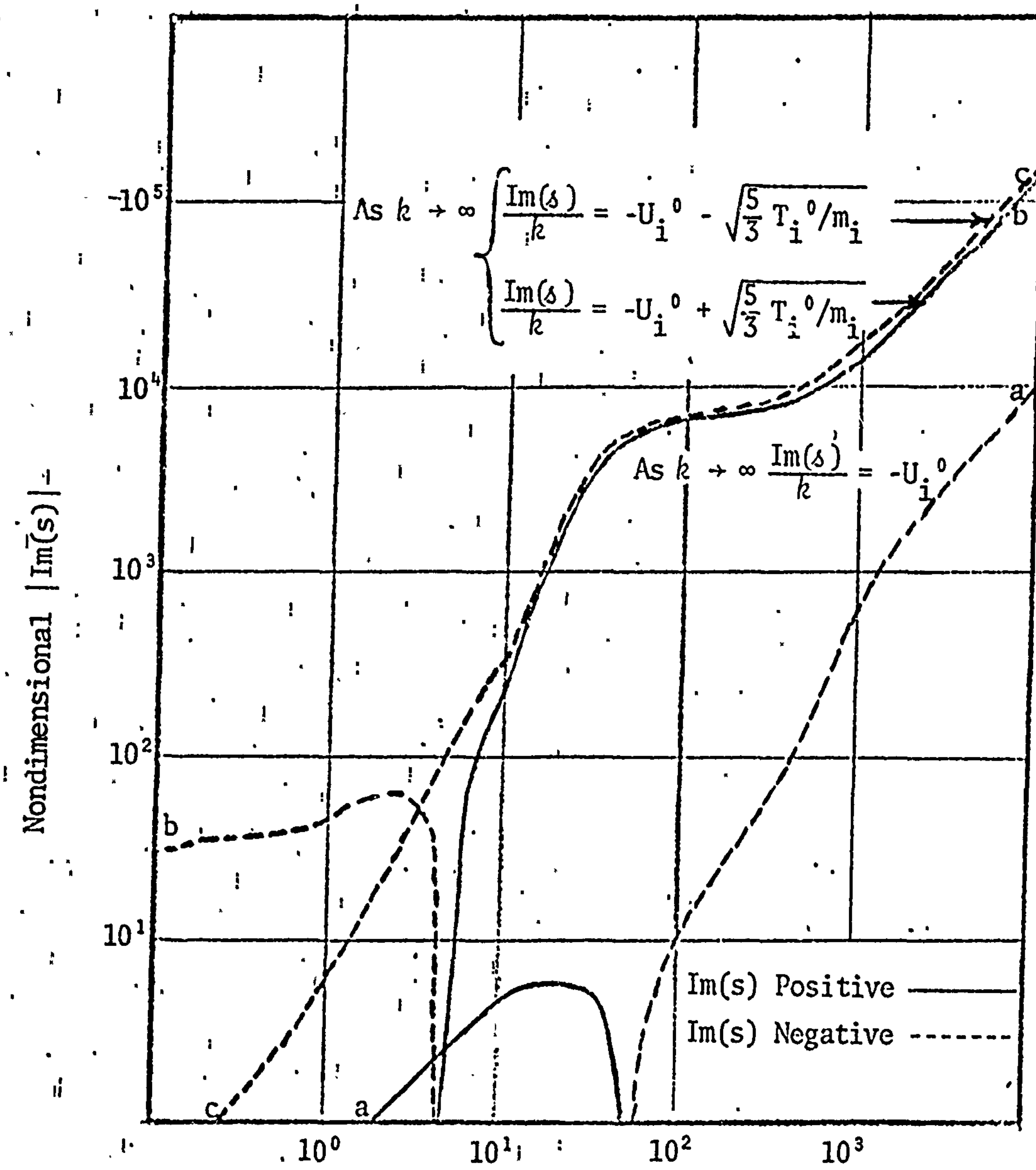

Figure 5. The Roots of the Dispersion Relation (Im(s) vs k) for the Section II Model with $\nu_- = \nu_-(E)$ (Mercury-in-Argon at 3 Torr)

50 m/sec and -50 m/sec respectively. The striations in the experiment are neutrally damped and occur over a narrow range of frequencies (Ref 11: 383). While backward waves over a narrow range of frequencies are predicted by the model, the group and phase velocities predicted are of the same order of magnitude but not approximately of equal magnitude as indicated in the experiment. Additionally, the damping predicted by the model does not show up in the experiment.

The Results of Other Theories

Figs. 6 and 7 compare the real and imaginary parts respectively of the striation roots of three different models for the same mercury-in-argon case depicted in Figs. 4 and 5. Root d is computed exactly as root b except that ν_- is held constant with respect to E rather than considered proportional to $E^{\frac{1}{2}}$ as in root b. Root d is included for two reasons. It illustrates the effect of the additional assumption $\nu_- \propto E^{\frac{1}{2}}$ when compared with root b and compares favorably in the region of striation-like behavior with root e computed by Swain and Brown's model (Ref 12: 1383-1386). Root f is computed by the Pekarek theory as detailed in Lee *et al.* (Ref 11: 381, 382).

Roots d and e predict neutrally damped waves with amplification per cycle of .457 and .828 respectively. Root f predicts exponentially growing waves with an amplification per cycle of 2.79. Striation frequency and wavelength at the points of maximum amplification are 3.5 khz and 2.1 cm for root d, 3.58 khz and 2.1 cm for root e, and 6.3 khz and 1.34 cm for root f. The corresponding group and phase velocities for roots d, e, and f are respectively 80.6 m/sec and -81 m/sec, 79 m/sec and -89 m/sec, and 84.5 m/sec and -35 m/sec. The sharp peak in each root

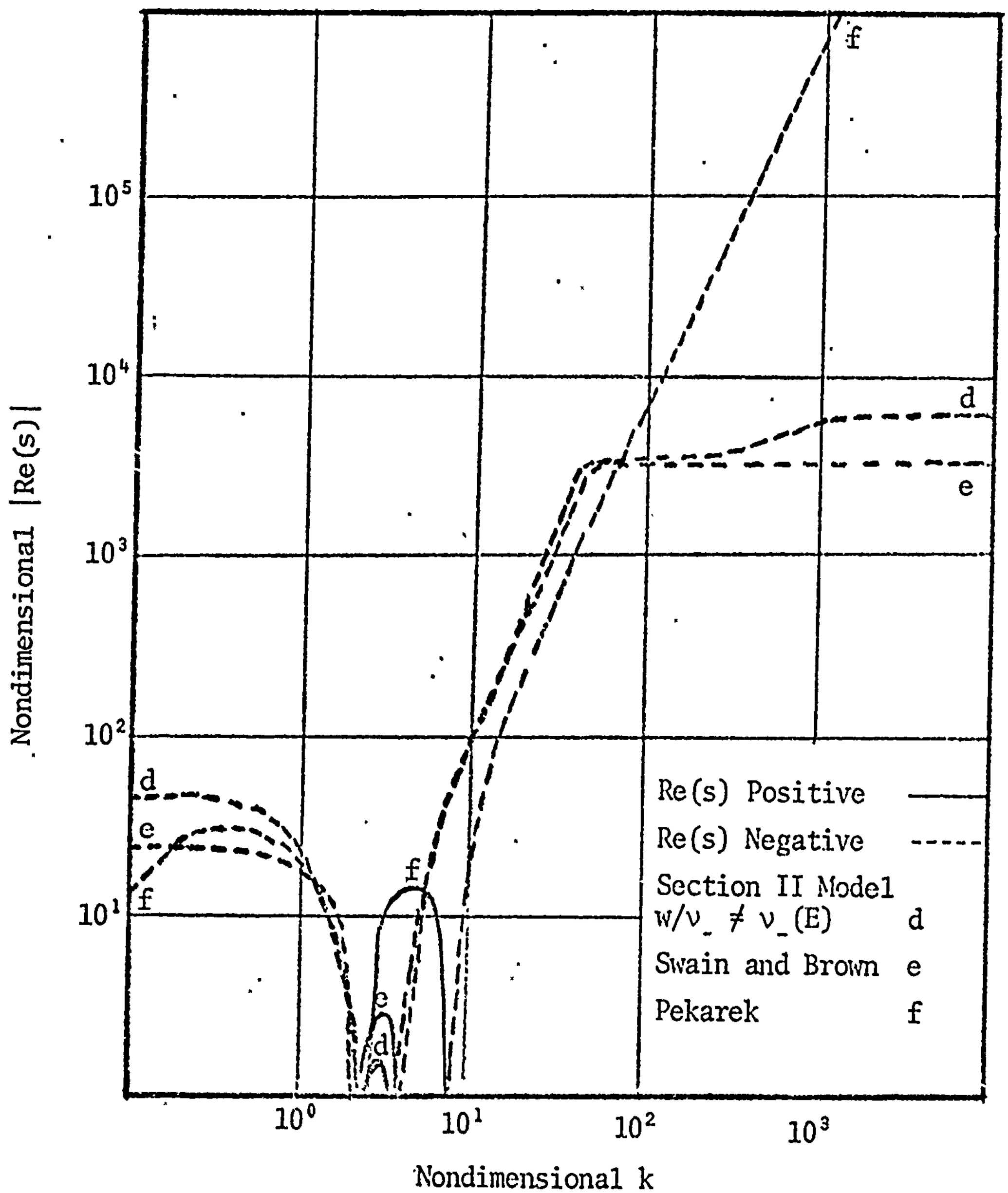

Figure 6. The Wave-like Root of the Dispersion Relations (Re(s) vs k) for Different Theories (Mercury-in-Argon at 3 Torr)

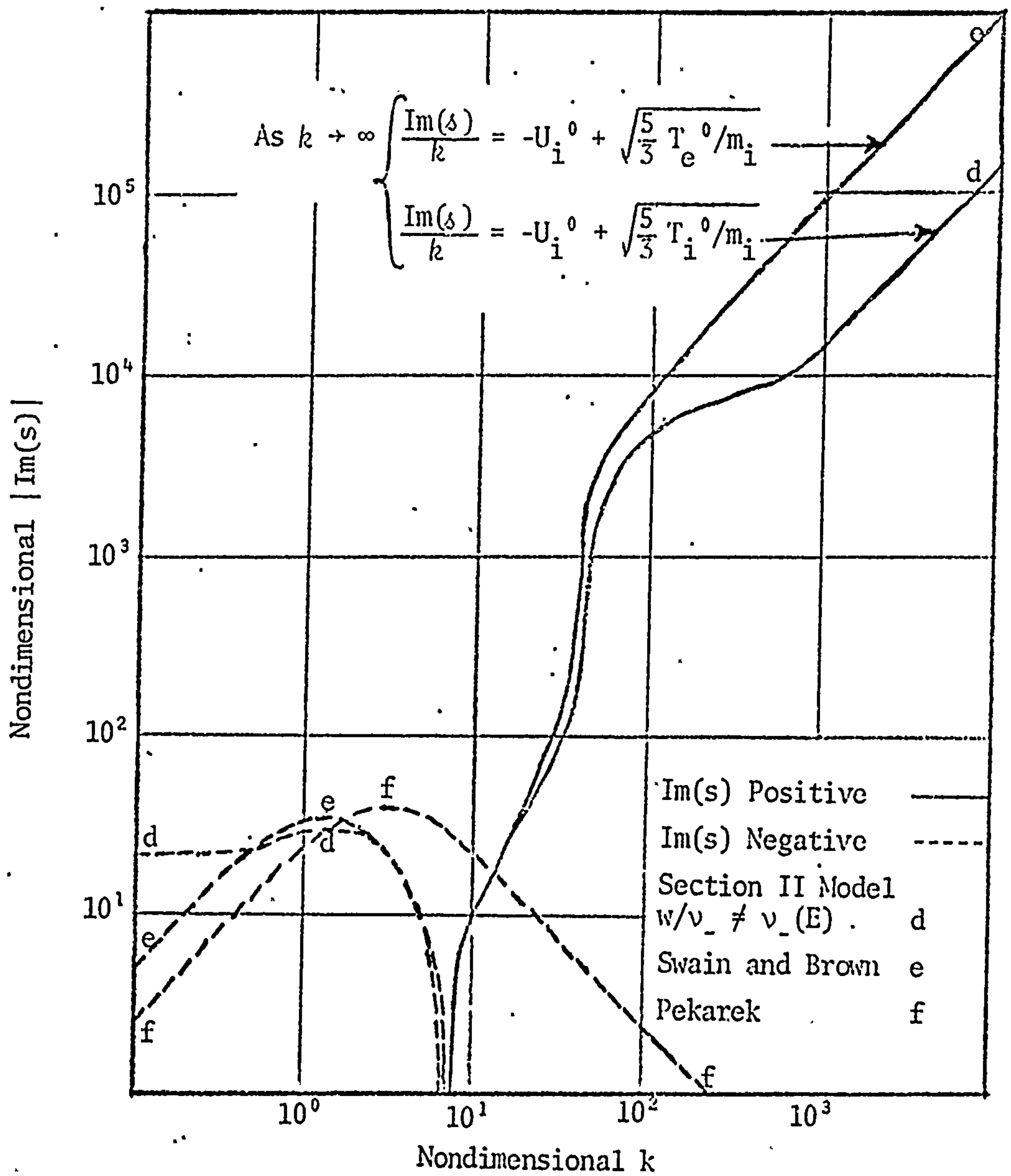

Figure 7. The Wave-like Root of the Dispersion Relations (Im(s) vs k) for Different Theories (Mercury-in-Argon at 3 Torr)

indicates a rather narrow range of frequencies for which wave propagation is allowed. The results predicted by the Section II model with $\nu_- \neq \nu_-(E)$ and the Swain and Brown model are very similar. Both agree well with experiment predicting neutrally damped backward waves over a n. rrow frequency band with group and phase velocities of approximately equal magnitude. The Pekarek theory predicts growing backward waves over a narrow frequency band with phase and group velocities of unequal but of the same order of magnitude.

The Characteristic Behavior for Large k

The characteristic behavior of the equations can be seen in the large k limit of the imaginary parts of roots a, b, and c in Fig. 4. Such behavior is expected since for variation of the form $\exp(ikx + st)$ Eq (46) becomes

$$(\lambda ik + s)V_i B_{ij} y_i = V_i F_i \tag{91}$$

As $k \to \infty$ the right hand side of Eq (91) becomes negligibl. . th respect to the left hand side; hence

$$(\lambda ik + s)V_i B_{ij} y_i \simeq 0 \tag{92}$$

$$(\lambda ik + s)^m \simeq 0 \tag{93}$$

$$\frac{i\mathrm{Im}(s) + \mathrm{Re}(s)}{ik} \simeq \frac{\mathrm{Im}(s)}{k} \simeq -\lambda = -v_p \ . \tag{94}$$

As k gets large the phase velocities for roots a, b, and c respectively approach $+U_i^0$, $+U_i^0 - \sqrt{\frac{5}{3} T_i^0/m_i}$, and $+U_i^0 + \sqrt{\frac{5}{3} T_i^0/m_i}$. In contrast, root e in Fig. 7, based on Swain and Brown's model which assumes $T_i = 0$ and

$N_i = N_e$ throughout, has a v_p in the large k limit of $+U_i{}^0 - \sqrt{\frac{5}{3} T_e^0/m_i}$. Swain and Brown's other root (not pictured) has a phase velocity of $+U_i{}^0 + \sqrt{\frac{5}{3} T_e^0/m_i}$ as $k \to \infty$. Both roots b and c initially parallel their corresponding Swain and Brown roots; however, at k $\simeq$ 30 the difference in N_i and N_e as expressed by Poisson's equation becomes large enough to separate the roots of the two different models toward their separate asymptotic paths.

Additional Comments

Results obtained by applying the Section II model to numerous other discharge conditions were generally similar to those discussed for the mercury-in-argon case above. In particular good qualitative agreement was obtained with both the Pekarek theory predictions and the results of the experiment described for the 50 Torr neon diffuse discharge case described in an article by Garscadden and Lee (Ref 13: 578). The Section II model did not predict striation-like behavior for the 35 Torr argon diffuse discharge case discussed in the same article. However, when the fraction of energy transferred in electron neutral collisions κ was considered constant with respect to E or $\nu_{e_0} \neq \nu_{e_0}(E)$, the predictions of the model were in much better agreement with both the Pekarek theory and experiment. The overall effect of letting ν_{e_0} and ν_- vary with E is to increase the damping in the root containing the striation-like behavior. The striation-like behavior in the majority of cases other than the one for mercury-in-argon discussed here appeared in the root whose large k phase velocity approaches $U_i{}^0$ rather than $U_i{}^0 - \sqrt{\frac{5}{3} T_i^0/m_i}$ as in root b, Fig. 4. The cause of such behavior and whether there is any corresponding physical significance has yet to be resolved.

IV. Conclusions

Because of the oversimplification of the physics involved and the small amount of data available from the actual experiments modeled, any comparison made between the results predicted by any of the models discussed herein and those of experiment must be highly qualitative. In this highly qualitative sense, the predictions of all the models discussed in the results agree moderately well with experiment. The better agreement with experiment obtained by the Section II model with $\nu_- \neq \nu_-(E)$ (root d) and by Swain and Brown's model (root e) than by the Section II model with $\nu_- = \nu_-(E)$ (root b) indicates that for the 3 Torr mercury-argon discharge μ_- is perhaps better approximated as constant rather than proportional to $E^{-\frac{1}{2}}$. Tending to confirm the above equilibrium data in Brown (similar data for an arbitrary gas is depicted in Fig. 2) unlike that in Von Engle (see Table I) indicates that this discharge condition is not quite such that μ_- can be considered proportional to $E^{-\frac{1}{2}}$, and that μ_- is in fact almost constant with respect to E for this operating region (Ref 4: 55).

As mentioned in Section III, the Section II model produced a similar but more damped behavior when ν_- and ν_{e0} were allowed to vary with E than when they were held constant. This seems physically consistent in both cases. In the ν_- case the effects of a small change in local E would be partially offset by the effects of a corresponding change in local mobility. In the ν_{e0} case the effects of a small change in the local fraction of energy transferred due to a small change in E would hasten an opposing change in electron temperature and hence electric field. The disagreement of experimental results with severe damping predicted by the Section II model for the briefly discussed 35 Torr argon case was probably caused by the use of too large a value for $\dot{\kappa}$ when computing the dispersion relation. The fact that better results were predicted when ν_{e_0} was held constant with respect to E indicates that $\dot{\kappa}$ cannot be reasonably inferred from equilibrium changes in κ with respect to E (see Table I). It is hoped that using a more reasonable value for $\dot{\kappa}$ will, in the future, provide better results for discharge conditions where inelastic electron neutral collisions are important; however, for the purpose of this report the Section II model containing the assumption that $\nu_{c_0} = \nu_{e_0}(E)$ based on the above method of obtaining $\dot{\kappa}$ is useful only in inferring the possible effects of such variation on ionization waves.

The fact that all models examined predict striation-like behavior in region from k = 3 to k = 5 for the 3 Torr mercury-in-argon case indicates that they are generally consistent with each other. This is not surprising since they are all based on some linearized form of the moment equations. For the cases examined the Section II model with $\nu_- \neq \nu_-(E)$ and $\nu_{e_0} \neq \nu_{e_0}(E)$ and the Swain and Brown model predict results which are in the best agreement with experiment. Solving the moment equations by not assuming $N_i = N_e$ and T_i to be negligible is of some interest from a mathematical point of view. However, the fact that Swain and Brown's model which includes these assumptions and the Section II model with $\nu_- \neq \nu_-(E)$ and $\nu_{e_0} \neq \nu_{e_0}(E)$ which does not include these assumptions predict almost identical striation behavior (roots d and e), indicates that the more complicated cubic dispersion relation Eq (87) obtained in the case of Section II model offers little advantage over the simpler quadratic dispersion relation obtained by Swain and Brown.

Bibliography

1. Rose, D. J. and M. Clark, Jr. Plasmas and Controlled Fusion. New York: The M.I.T. Press, 1961.

2. Von Engle, A. Ionized Gasses. London: The Oxford University Press, 1965.

3. Pekarek, L. and K. Rohlena. "The Influence of the Electron Temperature Gradient on the Space-Charge Field in a D.C. Discharge." Czechoslovak Journal of Physics, B 17: 856-866 (1967).

4. Brown, S. C. Basic Data of Plasma Physics. New York: The Technology Press of M.I.T., 1959.

5. von Misses, R. Mathematical Theory of Compressible Fluid Flow. New York: Academic Press, 1958.

6. Pekarek, L. and V. Krejci. "Theory of Moving Striations in Plasma of D.C. Discharge I. Basic Equations and Its General Solution." Czechoslovak Journal of Physics, B 12: 450-460 (1962).

7. Goodman, A. W. Modern Calculus with Analytic Geometry Volume II. London: The Macmillan Company Collier-Macmillan Limited, 1968.

8. Lee, D. A. "Nonlinear Macro-Oscillations in Plasmas Section I." Unpublished Notes 1-19, Wright-Patterson Air Force Base, Ohio: Aerospace Research Laboratories, May 1970.

9. Pekarek, L. and V. Krejci. "The Physical Nature of the Production of Moving Striations in a D-C Discharge Plasma." Czechoslovak Journal of Physics, B 11: 729-742 (1961).

10. Pekarek, L. and V. Krejci. "The Theory of Moving Striations in a D-C Discharge Plasma II. High Current Approximation." Czechoslovak Journal of Physics, B 13: 881-893 (1963).

11. Lee, D. A., P. Bletzinger, and A. Garscadden. "Wave Nature of Moving Striations." Journal of Applied Physics, 37: 377-387 (January 1966).

12. Swain, D. W. and S. C. Brown. "Moving Striations in a Low Pressure Argon Discharge." The Physics of Fluids, 14: 1383-1393 (July 1971).

13. Garscadden, A. and D. A. Lee. "Forward and Backward-wave Moving Striations in the Constricted Discharge." International Journal of Electronics, 20: 567-581 (1966).

14. Weissglas, P. and B. Andersson. "Ionization Waves in Semiconductors and Gaseous Plasmas." A report written under Air Force Contract AF 61(052)-888 sponsored by the Rome Air Development Center.

Appendix A

The Ionization Frequency Equation

Beginning with Von Engle's equation

$$\alpha = \frac{1}{N_e}\int_{\varepsilon_i}^{\infty} C_i(\varepsilon - \varepsilon_i) f_c N(\varepsilon) d\varepsilon \qquad (95)$$

where

$$N(\varepsilon)d(\varepsilon) = \left[\frac{2N_e}{\sqrt{\pi}}\left(\frac{\varepsilon}{\varepsilon_m}\right)^{\frac{1}{2}} e^{-\frac{\varepsilon}{\varepsilon_m}} d\left(\frac{\varepsilon}{\varepsilon_m}\right)\right] \qquad (96)$$

$$f_c = \sqrt{\frac{2\varepsilon}{m_e}}/\lambda_e \qquad (97)$$

$$\varepsilon_i = q_0 V_i \qquad (98)$$

$$\varepsilon_m = T_e \qquad (99)$$

$$C = \frac{Ap_0}{q_0}\lambda_e \qquad (100)$$

and ε is energy (Ref 2: 293), the ionization frequency α becomes

$$\alpha = Ap_0\sqrt{8/m_e\pi}\,\varepsilon_m^{-\frac{3}{2}}\int_{\varepsilon}^{\infty}(\varepsilon - \varepsilon_i)\varepsilon e^{-\frac{\varepsilon}{\varepsilon_m}} d\varepsilon \qquad (101)$$

Letting $\varepsilon = \varepsilon_i + X$, Eq (100) reduces to

$$\alpha = \frac{Ap_0}{q_0} \sqrt{8/m_e\pi}\ \varepsilon_m^{\frac{3}{2}} e^{-\frac{\varepsilon_i}{\varepsilon_m}} \int_0^\infty X(\varepsilon_i + X) e^{-\frac{X}{\varepsilon_m}} dX \tag{102}$$

or

$$\alpha \simeq Ap_0 \sqrt{8q_0/m_e\pi}\ V_i^{\frac{3}{2}} \left(\frac{q_0 V_i}{T_e}\right)^{\frac{1}{2}} e^{-\frac{q_0 V_i}{T_e}} \tag{103}$$

where V_i is the ionization potential in volts and A is the slope of the ionization efficiency curve in units of ion pairs/m/Torr/volt.

Appendix B

Sample Calculation of the Discharge Equilibrium Conditions for the 3 Torr Mercury-in-Argon Case Discussed in Section III

Values for N^0 and T^0 are assumed based on typical discharge conditions to be

$$N^0 = 10^{16}\ m^{-3}$$

$$T^0 = 5.52 \times 10^{-21}\ (400°K)$$

R, p_0, E^0 and $T_e{}^0$ from the experiment modeled (Ref 11: 383) are

$$R = .01\ m$$

$$p_0 = 3\ Torr$$

$$E^0 = 180\ volt/m$$

$$T_e{}^0 = 2.08 \times 10^{-19}\ joules$$

The mercury-in-argon mobility $\mu_0{}^+$ at 300°K and 760 Torr taken from Brown (Ref 4: 77) is

$$\mu_0{}^+ = .00018\ m^2/volt/sec$$

$\mu_0{}^+$ corrected to 400° and 3 Torr is

$$\mu^+ = .0605\ m^2/volt/sec$$

From Eqs (9) and (11)

$$\nu_+ = \frac{q_0}{m_{Hg^{++}}} = 7.7 \times 10^6 \text{ sec}^{-1}$$

From Eq (9)

$$U_i^{\,0} = \mu_+ E^0 = 10.8 \text{ m/sec}$$

From Eq (90)

$$\nu_{i_0} = 2.1 \times 10^7 \text{ sec}^{-1}$$

From Eq (75)

$$T_i^{\,0} = \frac{q_0 E^0 U_i^{\,0}}{\nu_{i_0}} + T_0$$

$$T_i^{\,0} = 5.53 \times 10^{-21} \text{ joules}$$

From Von Engle (see Table I) for electrons in argon

$$U_e^{\,0} = -4 \times 10^3 \text{m/sec}$$

and for mercury

$$V_i = 10.4 \text{ volts}$$

From Eq (11)

$$\nu_- = -\frac{E^0 q_0}{m_e U_e^{\,0}} = 7.9 \times 10^{-9} \text{ sec}^{-1}$$

From Eq (13)

$$\nu_{e_0} = -\frac{q_0 U_e{}^0 E^0}{T_e{}^0} = 5.53 \times 10^5\ \text{sec}^{-1}$$

From Eqs (4), (5), (7) and (8)

$$\alpha = (2.4/R)^2\,\frac{\mu_+ T_e{}^0}{q_0} = 4.7 \times 10^3\ \text{sec}^{-1}$$

Differentiating Eq (6) with respect to T_e and evaluating at $T_e = T_e{}^0$,

$$\alpha' = \frac{\alpha}{T_e{}^0}\left(\frac{q_0 V_i}{T_e{}^0} + \frac{1}{2}\right) \qquad (104)$$

$$\alpha' = 1.92 \times 10^{23}\ \text{sec}^{-1}\ \text{joules}^{-1}$$

From Eq (58)

$$\tau = \frac{2}{\alpha} = 4.25 \times 10^{-4}\ \text{sec}$$

Vita

Robert S. McCulloch was born 5 November 1944 in Staten Island, New York. He graduated from high school in Maryville, Tennessee in 1962, and received the degree of Bachelor of Science and a commission in the USAF from the United States Air Force Academy in 1967. He then served for three years as a pararescue officer with the Aerospace Rescue and Recovery Service.

Permanent address: 311 Broady Lane
Maryville, Tennessee 37801